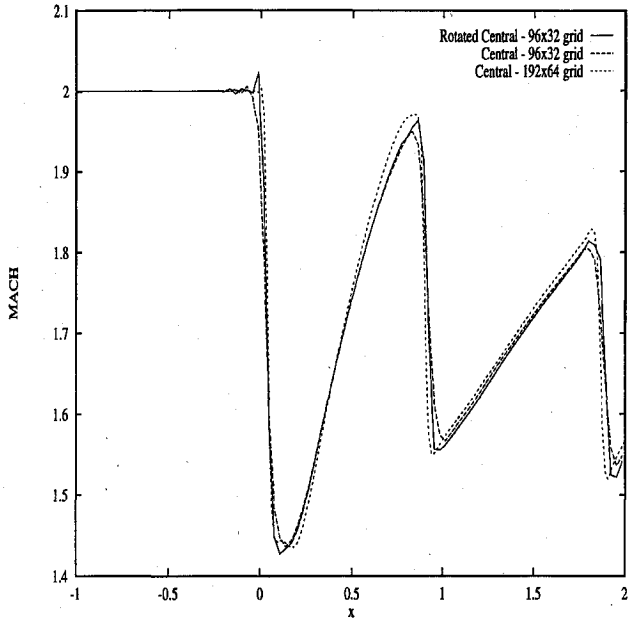

Fig. 3 Supersonic ramp, Mach number distribution at middle height of the channel.

not produce excessive smearing. This interesting property is fully exploited by analyzing Fig. 3 where the Mach-number distributions at middle height of the channel are presented. To assess the accuracy of the new procedure, we compare the results with the calculation performed with the standard scheme on a very fine grid (192 × 64 cells).

The standard central scheme (Fig. 2a) smears the first oblique shock as it approaches the upper wall. There is a large increase of the spreading in the resolution of the second and third reflected shocks. The introduced diffusion destroys the normal shock on the upper surface, and an oblique reflection practically occurs (there is no subsonic zone downstream of the shock). The shock thickness is reduced and shock reflections are better defined by using the new rotated scheme (Fig. 2b).

These improvements are clearly presented in Fig. 3. Sharp shocks are computed by the rotated technique and compared to the highly spread discontinuities of the standard central approach. This result is attributable to the resolution of shocks that are described by two inner cells, i.e., the same accuracy obtainable in case of grid-aligned discontinuities. The shock thickness is now comparable with the solution obtained by using the standard scheme over the refined grid.

As mentioned, the plots of Fig. 2 can be directly compared with previous results.[1] The reported scheme is a first-order rotated upwind that uses two Riemann solutions (in the dominant and in the minor directions) to build up the numerical dissipation. The flow-angle direction used in this case is the velocity magnitude gradient, but because of the numerical noise in regions of uniform flow (convergence halts at some error level), this has been limited.[1] That solution is comparable to that obtained with the present central rotated scheme, which is much simpler and more robust.

Acknowledgment

This work was carried out under cooperation between the Centro Italiano Ricerche Aerospaziali and the University of Naples in the framework of the ENFLOW project (Contract No. 940584).

References

[1]Van Leer, B., "Progress in Multidimensional Upwind Differencing," *Lecture Notes in Physics*, Vol. 414, Springer–Verlag, Berlin, 1992, pp. 1–26.

[2]Jameson, A., "Iterative Solution of Transonic Flow over Airfoils, Including Flows at Mach 1," *Communications on Pure and Applied Mathematics*, Vol. 27, 1974, pp. 283–309.

[3]Van Leer, B., Levy, D. W., and Powell, K. G., "Use of a Rotated Riemann Solver for the Two-Dimensional Euler Equations," *Journal of Computational Physics*, Vol. 106, No. 10, 1993.

[4]Dadone, A., and Grossman, B., "Characteristic-Based, Rotated Upwind Scheme for the Euler Equations," *AIAA Journal*, Vol. 30, No. 9, 1992, pp. 2219–2226.

[5]Paillere, H., Van der Weide, E., and Deconink, H., "Multidimensional Upwind Methods for Inviscid and Viscous Compressible Flows," Lecture Series 1995-02, von Kármán Inst. for Fluid Mechanics, Brussels, Belgium, 1995.

[6]Jameson, A., "Transonic Flow Calculations," Mechanical Engineering Dept., MAE Rept. 1651, Princeton Univ., Princeton, NJ, 1983.

[7]Swanson, R. C., and Turkel, E., "On Central Difference and Upwind Scheme," *Journal of Computational Physics*, Vol. 101, No. 2, 1992.

Modeling Mass Entrainment in a Quasi-One-Dimensional Shock Tube Code

C. J. Doolan* and P. A. Jacobs†
University of Queensland, Brisbane 4072, Australia

Introduction

QUASI-ONE-DIMENSIONAL simulations have been shown to provide quite detailed information about the transient gas-dynamics occurring in reflected-mode shock tunnels.[1,2] These models do well in describing the compression process within a free-piston shock tube driver and also in computing the trajectory of the shock wave within a shock tube.[1] However, the speed of the contact surface is usually incorrect because typical boundary-layer models do not redistribute the mass from the core flow to the walls. In quasi-one-dimensional formulations, this can be done by implementing a mass-loss model to the core flow.

Tani et al.[2] apply a mass-loss model to a quasi-one-dimensional formulation by using a simple displacement thickness model. Only qualitative agreement was found as the boundary-layer thickness was underestimated for strong shock waves. More sophisticated approaches such as those of Sharma and Wilson[3] use axisymmetric, two-dimensional simulations of the unsteady Navier–Stokes equations to investigate laminar boundary-layer shock tube flow. Although these methods give satisfactory results, the required computational effort is high, even for the simple shock tube cases they simulate. Conversely, quasi-one-dimensional codes are an attractive tool for engineering design because of their lower computational requirements. Including a mass-loss model for accurate test time and shock speed predictions would provide a useful tool for the designer of shock and expansion tubes where knowledge of the contact surface trajectory is important. Here, it is assumed the test time is the difference between the times of arrival of the contact surface and the shock wave at the measuring station.

Mirels[4] has provided an approximate analytical solution to the shock tube boundary-layer problem. In this case, a steady solution was obtained by assuming that the shock and contact surface had reached their equilibrium positions (i.e., mass flow through the shock front equals mass loss into the boundary layer). This approach gave a solution where the shock speed was independent of the fill pressure. However, for design purposes Mirels' model requires a knowledge of the physical performance of the particular shock tube driver in question. Still, Mirels' results showed that power-law velocity profiles in integral type analyses could be used to describe the boundary layer in a shock tube.

In this Note a quasisteady mass-entrainment model for shock tube boundary layers, specifically for use in quasi-one-dimensional codes, is described. Using this model, we calculate shock tube test times for the turbulent regime.

Received Oct. 24, 1995; revision received Feb. 12, 1996; accepted for publication Feb. 13, 1996.

*Graduate Student, Department of Mechanical Engineering. Member AIAA.

†Lecturer, Department of Mechanical Engineering. Member AIAA.

Mass-Entrainment Model

By assuming that the boundary layer is small with respect to the tube radius, the mass flow rate within the boundary layer $\dot{m}$ can be approximated by

$$\dot{m} = \pi D \int_0^{\delta} \rho u \, \mathrm{d}y \tag{1}$$

where D, δ, ρ, u, and y are the tube diameter, boundary-layer height, density, velocity, and vertical height through the boundary layer, respectively. To evaluate this integral, the Howarth transformation[5]

$$(\rho \, \mathrm{d}y)_{\text{compressible}} = (\rho^* \, \mathrm{d}y)_{\text{incompressible}} \tag{2}$$

is used along with an assumed incompressible boundary-layer velocity profile. Here $\rho^* = \rho T / T^*$ is the reference density, evaluated at the Eckert reference temperature T^*. The boundary-layer mass flow rate equation now becomes

$$\dot{m} = \pi D \rho^* u_e \delta_i \int_0^1 \frac{u}{u_e} \, \mathrm{d}\left(\frac{y}{\delta_i}\right) \tag{3}$$

The subscripts e and i represent the flow external to the boundary layer and an incompressible boundary-layer solution, respectively. Laminar or turbulent incompressible boundary-layer velocity profiles can now be inserted into Eq. (3) to yield analytical solutions. Here, we will consider only the turbulent case.

In this model, a one-seventh power-law velocity profile is used to describe the turbulent shock tube boundary layer. It is also assumed that the incompressible turbulent boundary layer grows according to

$$\frac{\delta_i}{x_l} = \frac{k_{\text{turb}}}{Re^{\frac{1}{5}}} \tag{4}$$

where $k_{\text{turb}} = 0.375$ (see Ref. 6). Substitution into Eq. (3) gives an expression for the mass flow rate in the boundary layer at a given value of Re_{xl} as

$$\dot{m} = \tfrac{7}{8} \pi D \rho^* u_e k_{\text{turb}} x_l Re_{xl}^{-\frac{1}{5}} \tag{5}$$

where Re_{xl} is the Reynolds number based on reference conditions at the distance x_l. The quantity x_l in a quasisteady shock tube problem is defined as the distance an individual cell has traveled from its initial position. The viscosity is calculated from the Sutherland viscosity law.

By taking the derivative of Eq. (5), one can find the change in mass flow rate over a small increment of x_l as

$$\mathrm{d}\dot{m} = 0.7 \pi D \rho^* u_e k_{\text{turb}} Re_{xl}^{-\frac{1}{5}} \, \mathrm{d}x_l \tag{6}$$

Therefore, for a particular time step, over a particular cell of length $\mathrm{d}x_l$, the mass of gas captured by the boundary layer is given by $\mathrm{d}\dot{m} \times \mathrm{d}t$, where $\mathrm{d}t$ is the time step.

In previous quasi-one-dimensional shock tube modeling, a friction factor model has been used for viscous wall shear stress and heat transfer.[1,7] Here, this is replaced with momentum and energy loss terms derived using the same assumptions as the mass-loss model. The momentum term is obtained by evaluating the integral

$$\dot{Q}_{\text{loss}} = \pi D \int_0^{\delta} \rho u^2 \, \mathrm{d}y \tag{7}$$

Taking the derivative of the resulting expression with respect to x_l and substituting for common terms using Eq. (6) give

$$\mathrm{d}\dot{Q}_{\text{loss}} = 0.889 \, \mathrm{d}\dot{m} u_e \tag{8}$$

The turbulent energy loss term is obtained by evaluating the integral

$$\dot{E}_{\text{loss}} = \pi D \int_0^{\delta} \rho u h \, \mathrm{d}y \tag{9}$$

where it is assumed that the enthalpy h can be replaced by the Eckert reference enthalpy h^* as was done for density when deriving Eq. (3). It therefore follows that the flow-core energy lost to the turbulent boundary layer is

$$\mathrm{d}\dot{E}_{\text{loss}} = \mathrm{d}\dot{m} h^* \tag{10}$$

The procedure for numerical modeling is described in full by Jacobs.[1] Briefly, the volumes of gas that are in their respective initial states (i.e., initial gas in driver and shock tube) are divided into a number of control-mass cells that interact through an approximate Reimann solver. The quasisteady viscous loss terms derived in this Note are applied at each time step by computing the corresponding amounts of mass, momentum, and energy lost to the boundary layer based on the conditions in the core flow and then subtracting these losses from the total quantities in each cell.

Comparison to Experimental Results

A shock tube turbulent boundary layer was investigated by simulating the flow in the ARO, Inc., J shock tube.[8] The driver pressure ranged from 25 to 124 MPa with either hydrogen or helium as the driver gas for the simulations presented here. The initial pressure in the shock tube ranged from 689 to 3.45 kPa, and the gas was modeled as air in thermochemical equilibrium.

Simulation results are summarized in Fig. 1. Good agreement with the experimental data at all shock Mach numbers M_s was obtained. However, the simulations do not match individual data points because details of the exact driver gas conditions were not available. Figure 2 shows contours of the logarithm of density in (x, t) space for two cases with the same initial conditions but with different boundary-layer models. Figure 2a uses the friction factor model[1] that does not include mass-loss terms, and Fig. 2b uses the mass-loss model presented in this Note. In Fig. 2b the contact surface can be seen to be accelerating to the speed of the slowly decelerating shock wave (2.00 km/s) at the end of the shock tube. In contrast, the contact surface in Fig. 2a travels at approximately 1.68 km/s along the entire length of the shock tube. The shock trajectories shown in Fig. 2 are nearly identical even though two different models for boundary-layer momentum and energy loss were used in each case. As a test of the solution accuracy, the number of cells along the shock tube was increased from 400 to 800 cells for the case shown in Fig. 2. This caused a change in the resulting test time and shock speed of under 0.5%. Simulations were performed on both an IBM RISC System 6000 and an IBM PC DX4-100 with run times of 397 and 835 μs/cell/time step, respectively. Overall CPU time for a simulation was on the order of 3 h.

To check that the correct shock speed was being obtained, the shock tube facility described by Fuehrer[9] was investigated. The initial conditions in the driver tube were 57.5 MPa and 685 K, and

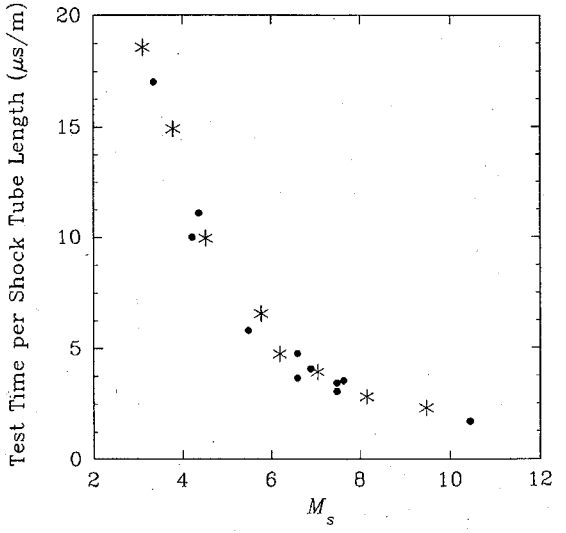

Fig. 1 Comparison of simulation results to the experimental results from Lacey[8]: •, experiment and ∗, simulation.

Table 1 Comparison of simulation shock speeds with experiment[9]

Distance from diaphragm, m	Simulation, km/s	Experiment, km/s
9.35	3.00	2.92
11.64	2.89	2.85
14.26	2.83	2.75

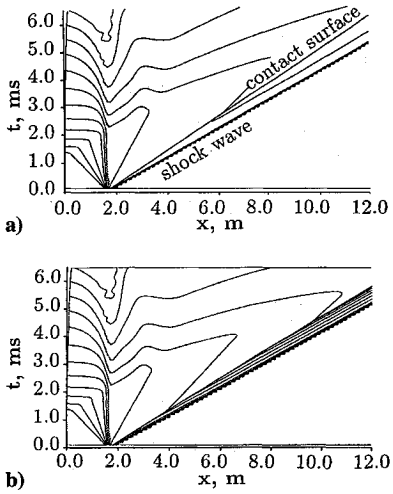

Fig. 2 Space–time diagrams comparing two different boundary-layer models; contours are equally spaced values of log ρ. In each case the driver gas was H_2, the shock tube initial pressure 206.7 kPa, and the diaphragm pressure ratio 445: a) the model without mass loss[1,7] and b) the present mass-loss model.

the gas was hydrogen. The shock tube was initially at 68.9 kPa and 296 K, and the gas was air in thermochemical equilibrium. Shock speed measurements were made along the length of the shock tube, and a comparison between the experimental data and the simulations was made in Table 1. Simulation and experiment differ in the range of 1–3%.

Concluding Remarks

By using fundamental boundary-layer theory, a model has been derived that can be used to provide shock tube test time and shock speed predictions. This model can be incorporated easily into a quasi-one-dimensional simulation code to provide a useful tool to the designer of shock and expansion tubes and gives accurate test time predictions for all turbulent flow shock tube cases tested.

Although they do not provide the depth of quality of information available in two-dimensional viscous codes, quasi-one-dimensional formulations can give adequate design information using a computationally less expensive approach. An adaptive one-dimensional mesh would aid the computational efficiency as, at this stage, the mass loss traps many cells with very little mass near the contact surface at long distances from the diaphragm ($L/D \approx 100$).

References

[1]Jacobs, P. A., "Quasi-One-Dimensional Modeling of a Free-Piston Shock Tunnel," *AIAA Journal*, Vol. 32, No. 1, 1994, pp. 137–145.

[2]Tani, K., Itoh, K., Takahashi, M., Tanno, H., Komuro, T., and Miyajima, H., "Numerical Study of Free-Piston Shock Tunnel Performance," *Shock Waves Journal*, Vol. 3, No. 4, 1994, pp. 313–319.

[3]Sharma, S. P., and Wilson, G. J., "Test-Times in Hypersonic Shock Tubes," AIAA Paper 95-0713, Jan. 1995.

[4]Mirels, H., "Shock Tube Test Time Limitation Due to Turbulent-Wall Boundary Layer," *AIAA Journal*, Vol. 2, No. 1, 1964, pp. 84–93.

[5]Watson, R. D., "Generalized Velocities in the Outer Region of Hypersonic Turbulent Boundary Layers," *AIAA Journal*, Vol. 17, No. 8, 1979, pp. 919–921.

[6]Schetz, J. A., *Boundary Layer Analysis*, Prentice–Hall, Englewood Cliffs, NJ, 1993, pp. 240, 241.

[7]Groth, C. P. T., Gottlieb, J. J., and Sullivan, P. A., "Numerical Investigation of High Temperature Effects in UTIAS-RPI Hypersonic Impulse Tunnel," *Canadian Journal of Physics*, Vol. 69, No. 7, 1991, pp. 897–918.

[8]Lacey, J. J., "Experimental Shock Tube Test Time—Turbulent Regime," *Proceedings of the 7th Shock Tube Symposium*, Univ. of Toronto Press, Toronto, ON, Canada, 1969, pp. 126–142.

[9]Fuehrer, R. G., "Measurements of Incident-Shock Test Time and Reflected Shock Pressure at Fully Turbulent Boundary-Layer Test Conditions," *Proceedings of the 7th Shock Tube Symposium*, Univ. of Toronto Press, Toronto, ON, Canada 1969, pp. 31–59.

Hyperbolic Equation Method of Grid Generation for Enclosed Regions

Yih Nen Jeng*
National Cheng Kung University, Tainan 70101, Taiwan, Republic of China
and
Yuan-Chang Liou†
Kung Shan Institute of Technology and Commerce, Tainan 70111, Taiwan, Republic of China

Introduction

In the recent past, two popular types of method for grid system generation have been developed.[1] The first type employs algebraic formulas, and the second type solves elliptical, parabolic, or hyperbolic partial differential equations.[1–8] Among the second type, the hyperbolic equation technique is very fast and has been extensively studied.[5–10]

Because of the open boundary constraint of the hyperbolic system, the classical hyperbolic equation method is not available for grid generation within enclosed regions. This limitation is partially removed by the combination methods of Refs. 9 and 10, which sum up grids generated from each boundary separately. However, combination methods require at least twice the CPU time as the original method.

In a recent study,[11] the authors combined the grid front marching method[12] and the parabolic equation method. In this study, a similar idea is applied to extend the Cordova and Barth hyperbolic equation method[13] to enclosed regions.

Formulation

Cordova and Barth[13] considered the following two equations to define the mapping between an irregular region on the x–y plane and a regular region on the ξ–η plane:

$$x_\xi x_\eta + y_\eta y_\xi = s_\xi s_\eta \cos\theta, \qquad x_\xi y_\eta - x_\eta y_\xi = s_\xi s_\eta \sin\theta \quad (1)$$

where $x_\xi = \partial x/\partial\xi$ and θ denotes the angle between two intersecting grid lines. Assuming that x^o and y^o along the grid level are known and x and y along an adjacent grid level are to be found, the grid equations can be linearized[5] into the following forms:

$$\boldsymbol{A}\boldsymbol{r}_\xi + \boldsymbol{B}\boldsymbol{r}_\eta = \boldsymbol{S}$$

$$\boldsymbol{A} = \begin{bmatrix} x^o_\eta & y^o_\eta \\ y^o_\eta & -x^o_\eta \end{bmatrix}, \qquad \boldsymbol{B} = \begin{bmatrix} x^o_\xi & y^o_\xi \\ -y^o_\xi & x^o_\xi \end{bmatrix} \quad (2)$$

$$\boldsymbol{S} = \begin{bmatrix} s_\xi s_\eta \cos\theta + s^o_\xi s^o_\eta \cos\theta^o \\ s_\xi s_\eta \sin\theta + s^o_\xi s^o_\eta \sin\theta^o \end{bmatrix}$$

Received Sept. 18, 1995; revision received Feb. 12, 1996; accepted for publication Feb. 12, 1996.

*Professor, Institute of Aeronautics and Astronautics. Member AIAA.
†Associate Professor, Department of Mechanical Engineering.